Origin of potential errors in the quantitative determination of terahertz optical properties in time-domain terahertz spectroscopy

Qijun Liang (梁启军)[1], Gregor Klatt[2], Nico Krauß[1], Oleksii Kukharenko[3], and Thomas Dekorsy[1,*]

[1]*Department of Physics and Center for Applied Photonics, University of Konstanz, 78464 Konstanz, Germany*

[2]*Laser Quantum GmbH, 78464 Konstanz, Germany*

[3]*Faculty of Physics, National Taras Shevchenko University of Kyiv, 01601 Kyiv, Ukraine*

**Corresponding author: thomas.dekorsy@uni-konstanz.de*

Received April 27, 2015; accepted June 19, 2015; posted online July 23, 2015

We demonstrate theoretically and experimentally how changes of a terahertz (THz) beam induced by the sample affect the accuracy of the determination of THz dielectric properties in THz time-domain transmission spectroscopy (TDTS). We apply a Gaussian beam and the ABCD matrix formalism to describe the propagation of the THz beam in a focused beam setup. The insertion of the sample induces a focus displacement which is absent in the reference measurement without a sample. We show how the focus displacement can be corrected. The THz optical properties after focus displacement correction reported in this Letter are in quantitative agreement with those obtained using collimated beam THz–TDTS in previous work.

OCIS codes: 300.6495, 160.4760, 120.7000.

doi: 10.3788/COL201513.093001.

Terahertz (THz) time-domain spectroscopy (TDS) has become an important approach to investigate the optical properties of various materials including semiconductors, oxides, solvents, and gases[1–5]. This technique requires measuring the time-domain electric field of the THz pulse after passing through the investigated sample in a transmission geometry setup. The complex frequency-domain spectra can be obtained through a Fourier transform, and the refractive index and absorption coefficient of the sample can be simultaneously obtained from the ratio of the spectra without applying Kramers–Kronig relations.

A transmission geometry setup is usually applied to investigate materials with good transparency in the THz frequency range. Many dielectrics and semiconductors such as quartz, Si, GaN, and GaAs have been characterized with high accuracy by using a collimated beam in THz time-domain transmission spectroscopy (TDTS)[6,7]. In a collimated beam, the diameter of the THz beam on the sample should have the same size as the parabolic mirrors. This requires large and homogeneous samples. A focused beam setup circumvents this problem because the THz beam can be tightly focused within the refraction limit onto the sample. However, a focus displacement induced by the sample will affect the accuracy of the obtained THz optical properties, because the THz spot in the detector crystal will change. Since the THz detection scheme in THz–TDS is not based on a detector that integrates the total received power, a THz spot increase will appear as absorption in the sample. Hence the influence on the quantitative values of the optical constants depends on the sample thickness. This focus displacement has been discussed by some groups previously[8,9]. In Ref. [8], highly accurate refractive indices of a set of materials were obtained by introducing Gouy shift corrections. In Ref. [9], the researchers presented the effect of the defocusing to THz–TDS analysis of silicon. However, the signal-to-noise ratio (SNR) is lower compared to our work and the effect on both the determination of the real and imaginary part is not quantitatively presented.

In this Letter, we analyze the effect of focus displacement to both the refractive index and the absorption coefficient, and demonstrate theoretical and experimental procedures to reduce the refocusing errors. We describe the propagation of the THz beam in a focused beam setup using a Gaussian beam and the ABCD matrix method[10]. The influence of the focus displacement on the evaluation of the refractive index and absorption coefficient is discussed theoretically. Furthermore, we determine the optical properties of a high-resistivity GaAs wafer, which are carefully measured in the focused beam THz–TDTS setup with and without focus displacement correction, respectively. The experimental correction exhibits good agreement with the theoretical evaluation, which is further verified by measurements using a collimated beam THz–TDTS setup in previous work[7].

Our THz–TDS system is based on asynchronous optical sampling (ASOPS), which relies on two mode-locked Ti:sapphire femtosecond lasers with repetition rates of approximately 1 GHz[5,11]. The repetition rate offset of the two lasers is stabilized to be 4 kHz by a phase-locked loop. One laser with higher repetition rate serves as pump laser for excitation of the THz emitter, and the other laser with lower repetition rate serves as probe laser for electro-optic detection. The THz radiation is generated in a micro-structured large-area photoconductive THz emitter[12] and is collected and collimated by 90° off-axis parabolic mirrors, and finally focused onto a (110) ZnTe detector crystal[13]. The probe beam is overlaid with the THz beam on the detector crystal and experiences a polarization change due to the electro-optic effect induced by the THz electric field. The time-domain data of the sample and reference are obtained by measuring with and without the sample in the THz beam path, respectively. Our experimental setup can be simplified by modeling the off-axis parabolic mirrors as thin lenses with focal length f (Fig. 1). The distance between the parabolic mirrors is set to be $2f$, which is the optimized separation for the best image of the THz pulse[14].

After placing a homogenous sample in the beam path of the setup shown in Fig. 1(a), the focus position will be shifted by $\Delta = d(n-1)/n$, where Δ is focus displacement, d and n are the thickness and the refractive index, respectively, of the sample. In this case, the THz focus volume within the detector crystal will not be at the minimum as that without a sample in the beam path. Therefore, the focus displacement will introduce inaccuracy in the determination of the quantitative optical properties of the sample.

To ensure that the beam waist is in the middle position of the sample and to retain the symmetry of the setup, the positions of the sample and the components afterwards are shifted by $\Delta/2$ and Δ in the z direction, respectively [Fig. 1(b)]. Because the variation of the refractive index n of GaAs is less than 1.0% in the full investigated THz frequency range (0.2–3.0 THz), which will be illustrated in a subsequent paragraph, we treat n as constant ($n = 3.60$) when we carry out the experimental correction.

The THz pulse can be modeled as a Gaussian beam. Within the paraxial-ray approximation, the propagation of the Gaussian THz pulse in free space can be described by[15]

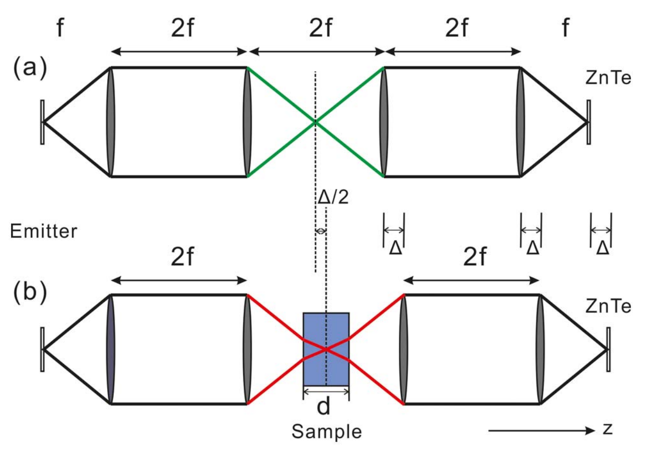

Fig. 1. Scheme of the experimental setup: (a) without focus displacement correction and (b) with focus displacement correction.

$$\vec{E}(r,z,\nu) = \vec{E}_0 \frac{w_0}{w(z)} \exp\left\{-i[kz - \Psi(z)] - r^2\left[\frac{1}{w^2(z)} + \frac{ik}{2R(z)}\right]\right\}, \quad (1)$$

where $\vec{E}_0$ and w_0 are the electric field and the radius of the THz pulse at $z = 0$, respectively.

The radius of the beam, the radius of the curvature, the Rayleigh length, and the Gouy shift can be expressed as

$$w^2(z) = w_0^2\left(1 + \frac{z^2}{z_0^2}\right),$$
$$R(z) = z\left(1 + \frac{z_0^2}{z^2}\right),$$
$$z_0 = \frac{\pi w_0^2 \nu}{\mathrm{c}},$$
$$\Psi(z) = \arctan\left(\frac{z}{z_0}\right), \quad (2)$$

where ν is the frequency, and c is the speed of light in vacuum.

The emitter and the detector can be treated as infinitely thin compared with the focus length f, and consequently the dielectrics of the THz emitter and the detector crystal are not taken into account in the simulation. In accordance with the q parameter of the Gaussian beam and the ABCD matrix[10], we compare the beam radius in the middle position of the sample and the detector crystal between the two setups (Fig. 1) without taking into account the effect of the finite aperture of the lens which will be taken into account in a subsequent paragraph.

When there is no sample in the THz beam path [Fig. 1(a)], the beam radius at the focus position ($z = 4f$) and the detector crystal ($z = 8f$) are equal to w_0, which means that the THz pulse is imaged without any distortion. However, if we place a homogeneous sample with refractive index n and thickness d into the beam path (the middle position of the sample is at $z = 4f$), the THz beam radius imaged by the detector crystal will be larger than in the reference. Here we define the setup as an "in-focus" or "off-focus" configuration, when the minimum THz spot size is or is not in the middle position of the sample and the detector crystal.

Table 1 shows the calculated beam radius in the middle position of the sample and the detector crystal in the

Table 1. Beam Radius in Off- and In-focus Configuration

Configuration	Position	$w(z)$
	$z = 0$	w_0
Off-focus	$z = 4f$	$\sqrt{n w_0^2 + \frac{(n-1)^2 d^2 \mathrm{c}^2}{4n\pi^2 w_0^2 \nu^2}}$
	$z = 8f$	$\sqrt{w_0^2 + \frac{(n-1)^2 d^2 \mathrm{c}^2}{n^2 \pi^2 w_0^2 \nu^2}}$
In-focus	$z = 4f + \Delta/2$	$\sqrt{n} w_0$
	$z = 8f + \Delta$	w_0

off- and in-focus configuration based on the ABCD law and infinite lens aperture assumption.

As shown in Table 1, in the off-focus configuration the beam radius in the middle position of the sample and the detector crystal depend on the frequency, the thickness, and the refractive index of the sample. From the expressions, we can expect that the beam radius in the middle position of the sample and the detector crystal increases with decreasing frequency and increasing sample thickness and refractive index. By implementing focus displacement correction [Fig. 1(b)], however, the beam radius is no longer frequency- and thickness-dependent.

When we deal with long wavelength waves such as those associated with THz radiation, the effect of the finite aperture of the lens should not be neglected. Assume that the spatial transmittance profile of the lens of diameter D is as follows[16]

$$T(r) = \exp\left(-\frac{4r^2}{D^2}\right). \tag{3}$$

In combination with Eq. (1), the beam radius at the lens ($z = f$, $3f$, $5f$, and $7f$) is transformed to be

$$\frac{1}{w'^2(z)} = \frac{1}{w^2(z)} + \frac{2}{D^2}. \tag{4}$$

Figure 2 shows the frequency and thickness dependence of the beam radius in the detector crystal in the off- and in-focus configuration. The diameter of the lens is 50.8 mm and the THz beam radius w_0 is set to be 150. In the off-focus configuration, the beam radius in the detector crystal depends on both the thickness and the frequency. In the in-focus configuration with focus displacement correction, however, the beam radius only depends on the frequency and is always smaller than that in the off-focus configuration. This means that the beam is more tightly focused in the in-focus configuration. The frequency

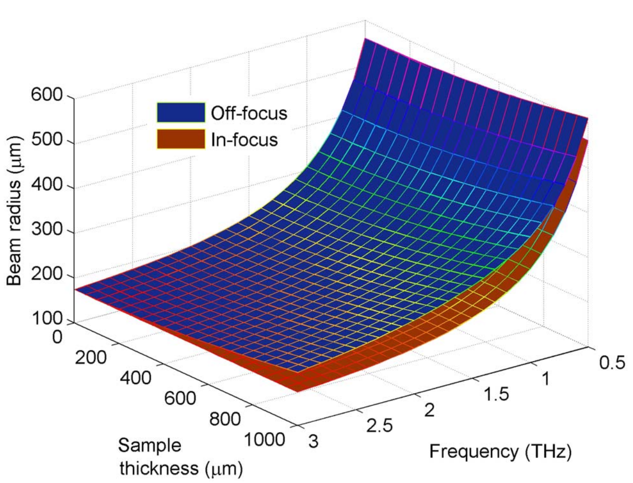

Fig. 2. Frequency and sample thickness dependence of the THz beam radius in the detector crystal in the off- and in-focus configurations.

dependence of the beam radius is mainly ascribed to the finite aperture of the lens.

With the usual evaluation method, the real refractive index n and absorption coefficient α of a sample can be calculated simply by the following formula if the imaginary part of the refractive index is much smaller than the real part[17]

$$n = 1 + \frac{|\Phi| c}{2\pi\nu d},$$
$$\alpha = -\frac{2}{d}\ln\left[\frac{(n+1)^2}{4n}|T|\right], \tag{5}$$

where $|\Phi|$ and $|T|$ are the phase shift and the amplitude transmission, respectively, of the sample with respect to the reference.

In Eq. (1), there are phase and amplitude terms influencing the evaluation of the refractive index and absorption coefficient as a focus displacement occurs. Let n_{true} and α_{true} be the true refractive index and absorption coefficient, respectively; n_{eval} be the refractive index evaluated directly from Eq. (5). Taking into account the focus displacement, we obtain the following between the true and the directly evaluated values

$$n_{\text{eval}} = n_{\text{true}} + \frac{c}{2\pi\nu d}\arctan\left[\frac{(n_{\text{true}}-1)d}{n_{\text{true}} z'_0}\right],\ z'_0 = \frac{\pi w_0'^2 \nu}{c},$$
$$\alpha_{\text{true}} = -\frac{2}{d}\ln\left\{\frac{(n_{\text{true}}+1)^2}{4n_{\text{true}}}|T|\left[\frac{1-\exp(-2r_0^2/w_0'^2)}{1-\exp(-2r_0^2/w'^2(z))}\right]^{\frac{1}{2}}\right\}, \tag{6}$$

where $r_0 \approx w'_0$ is the radius of the circle within which the power is integrated. $w'(z)$ and w'_0 are the THz beam radius in the detector crystal with and without a sample in the off-focus configuration, respectively. Comparing Eq. (6) with Eq. (5), we can see that the true value of the refractive index is always smaller than the value evaluated with the usual method, and the true absorption coefficient can be obtained by a modification term related to the THz beam radius in the detector crystal. Hence, the focus displacement correction can be made by measuring the sample in the off-focus configuration in combination with Eq. (6). It should be noted that the absorption coefficient correction is strongly affected by the overlap of the probe and THz beams in the detector crystal. This effect will be not pronounced if the sample is not too thick (i.e., $d < 300$ μm), because the THz field amplitude on the axis will not change too much. For thick samples, the effect will be reduced if most of the THz spot overlaps with the detecting probe beam, which requires a more tightly focused THz beam.

As aforementioned, the THz beam will be more tightly focused in the middle position of the sample and the detector crystal when we carry out a measurement using the in-focus configuration. Therefore, the focus displacement induced phase and amplitude terms influencing the evaluation of optical properties can be reduced, and then we can obtain a more accurate evaluation by use of Eq. (5). To carry out the focus displacement correction experimentally using the in-focus configuration, however, we must know the refractive index n of the sample in advance to calculate the displacement Δ. The procedure to measure an unknown sample using the in-focus configuration consists of three steps: (1) measure the sample in the off-focus configuration to estimate the average refractive index n; (2) shift the sample by $\Delta/2$, the last two parabolic mirrors (on a single moveable board), and the detector crystal by Δ in the z direction; (3) measure the sample in the in-focus configuration and evaluate the optical properties using the usual method.

Figure 3 shows the time-domain data and the frequency-domain spectra of high-resistivity (100) GaAs with a thickness of 990 μm, measured in the off- and in-focus configuration. The reference is measured without a sample in the beam path of the off-focus configuration. The displacement Δ in this case is around 715 μm. It should be noted that the displacement does not introduce an additional phase shift between the probe pulse and the THz pulse because the probe pulse travels collinearly with the THz pulse. It can be observed that the transmittance spectra from the in-focus configuration exhibit a somewhat higher transmission and smaller phase shift compared with those from the off-focus configuration.

Figure 4 illustrates the refractive index and absorption coefficient of GaAs obtained from the time-domain data. The experimental values are evaluated according to Eq. (5), with the data measured in the off- and in-focus configuration. The theoretical correction (green dash-dotted line) is performed, based on Eq. (6) in combination

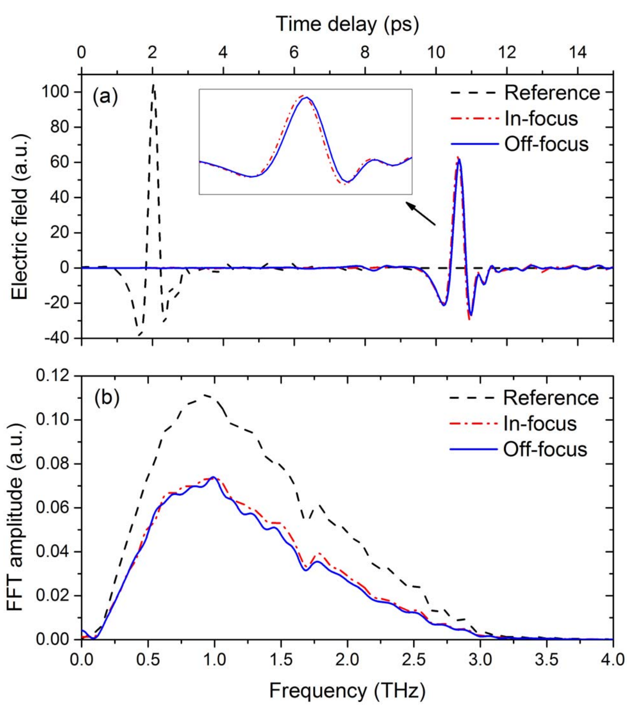

Fig. 3. THz-TDTS of high-resistivity (100) GaAs with a thickness of 990 μm in the off- and in-focus configuration: (a) time-domain data and (b) frequency-domain spectra.

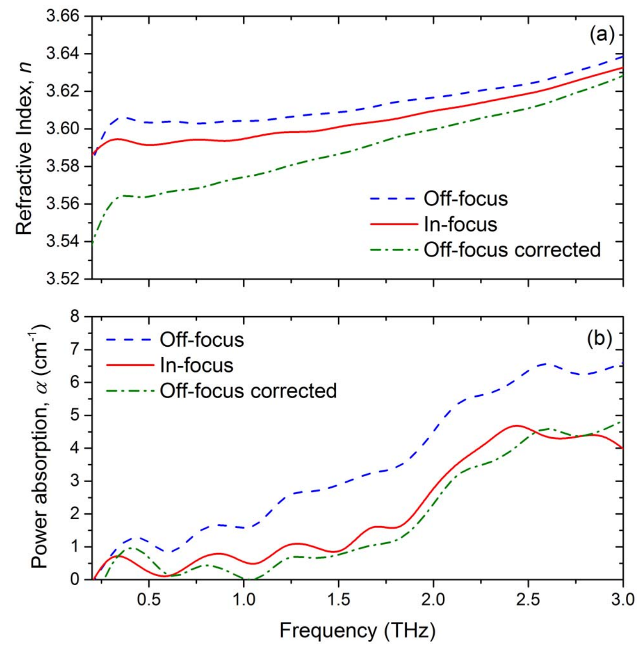

Fig. 4. Optical properties of high-resistivity GaAs in the THz frequency range: (a) refractive index and (b) absorption coefficient.

with the experimental data from the off-focus configuration. The values measured in the in-focus configuration (red solid line) are smaller than those measured in the off-focus configuration (blue dashed line) and larger than those with theoretical correction. For the refractive index, the difference is about 0.01 at 1 THz. For the absorption coefficient, the difference is more significant. From the off-focus measurement, we can see that the absorption coefficient increases monotonically with the frequency and almost approaches a constant value of 6 cm^{-1} from 2.4 to 3.0 THz. From the in-focus measurement, the power absorption is about 2 cm^{-1} smaller than the value measured in the off-focus configuration. In addition, the absorption increases slowly below 1.8 THz and rapidly above 1.8 THz, and then stops increasing after a feature at around 2.4 THz, which was also observed by Ralph *et al.*[18]. The absorption feature at around 2.5 THz in the off-focus configuration shows a small blue shift relative to that in the in-focus configuration, which is attributed to the relative larger defocusing effect at this frequency in the off-focus configuration. It should be noted that the modulation with 0.5 THz spacing below 1.8 THz in the absorption coefficient is a result of the limited time window chosen for the fast Fourier transform. The deviation between the experimental and theoretical focus displacement correction mainly stems from several limitations; for instance, the precision of the thickness of the sample, the modeling of the propagation of the lowest-order Gaussian THz beam and the parabolic mirrors, the assumption of constant n in the in-focus experiment and the infinite thin emitter and detector. Although not completely, the theoretical correction based on

Eq. (6) brings improvement to the precision of material characterization.

In addition, the refractive index and absorption coefficient of high-resistivity GaAs determined using our in-focus configuration are compatible with the values measured using a collimated beam THz–TDTS setup[7], which means that the deviation of the refractive index and absorption coefficient mainly stems from the focus displacement of the Gaussian beam.

In conclusion, we demonstrate theoretically and experimentally the influence of the focus displacement to material characterization in conventional focused-beam THz–TDTS. We apply the ABCD law to describe the propagation of a Gaussian THz pulse and calculate the beam radius in the detector crystal. Due to focus displacement, there are phase and amplitude terms that affect the evaluation of the refractive index and absorption coefficient. The beam radius in the detector crystal depends on the frequency, thickness, and refractive index of the sample. Ideally, the beam radius in the detector crystal in the in-focus configuration will be the same as the original beam radius if the aperture of all the lenses is infinite. However, the effect of the finite aperture of the lenses should be taken into account because of the large wavelength of THz radiation. By using the in-focus configuration, we can almost eliminate the effect of the thickness of the sample and achieve a more-precise material characterization.

The theoretical correction based on Eq. (6) can improve the evaluation compared with the usual evaluation method. In addition, the refractive index and absorption coefficient of high-resistivity GaAs measured in our in-focus configuration with focus displacement correction are compatible with the measurements using a collimated beam THz–TDTS setup in previous work.

We gratefully acknowledge the support from the Center for Applied Photonics (CAP) at the University of Konstanz, the DFG through the SFB 767 (Germany), and the China Scholarship Council (CSC).

References

1. J. Lloyd-Hughes and T.-I. Jeon, J. Infrared Millimeter Terahertz Waves **33**, 871 (2012).
2. R. Smith and M. A. Arnold, Appl. Spectrosc. Rev. **46**, 636 (2011).
3. A. K. Azad, J. Han, and W. Zhang, Appl. Phys. Lett. **88**, 021103 (2006).
4. J. Hunger, A. Stoppa, A. Thoman, M. Walther, and R. Buchner, Chem. Phys. Lett. **471**, 85 (2009).
5. G. Klatt, R. Gebs, C. Janke, T. Dekorsy, and A. Bartels, Opt. Express **17**, 22847 (2009).
6. W. Zhang, A. K. Azad, and D. Grischkowsky, Appl. Phys. Lett. **82**, 2841 (2003).
7. D. Grischkowsky, S. Keiding, M. van Exter, and Ch. Fattinger, J. Opt. Soc. Am. B **7**, 2006 (1990).
8. P. Kužel, H. Němec, F. Kadlec, and C. Kadlec, Opt. Express **18**, 15338 (2010).
9. F. D'Angelo, M. Bonn, and D. Turchinovich, in *Proceedings of the 38th International Conference on IRMMW-THz 2013* 6665505 (IEEE, 2013).
10. O. Svelto, *Principles of Lasers* (Plenum, 1998).
11. R. Gebs, G. Klatt, C. Janke, T. Dekorsy, and A. Bartels, Opt. Express **18**, 5974 (2010).
12. A. Dreyhaupt, S. Winnerl, T. Dekorsy, and M. Helm, Appl. Phys. Lett. **86**, 121114 (2005).
13. G. Gallot and D. Grischkowsky, J. Opt. Soc. Am. B **16**, 1204 (1999).
14. P. U. Jepsen, R. H. Jacobsen, and S. R. Keiding, J. Opt. Soc. Am. B **13**, 2424 (1996).
15. R. W. Ziolkowski and J. B. Judkins, J. Opt. Soc. Am. A **9**, 2021 (1992).
16. T. Hattori, R. Rungsawang, K. Ohta, and K. Tukamoto, Jpn. J. Appl. Phys. **41**, 5198 (2002).
17. L. Duvillaret, F. Garet, and J.-L. Coutaz, J. Opt. Soc. Am. B **17**, 452 (2000).
18. S. E. Ralph and D. Grischkowsky, Appl. Phys. Lett. **60**, 1070 (1992).